**Advances in Nano Research**, *Vol. 10, No. 2 (2021) 129-138*
DOI: https://doi.org/10.12989/anr.2021.10.2.129


# Monitoring and control of multiple fraction laws with ring based composite structure

Mohamed A. Khadimallah*[1,2], Muzamal Hussain[3], Muhammad Nawaz Naeem[3], Muhammad Taj[4] and Abdelouahed Tounsi[5,6]

*[1]Prince Sattam Bin Abdulaziz University, College of Engineering, Civil Engineering Department, BP 655, Al-Kharj, 16273, Saudi Arabia*
*[2]Laboratory of Systems and Applied Mechanics, Polytechnic School of Tunisia, University of Carthage, Tunis, Tunisia*
*[3]Department of Mathematics, Govt. College University Faisalabad, 38000, Faisalabad, Pakistan*
*[4]Department of Mathematics, University of Azad Jammu and Kashmir, Muzaffarabad, 1300, Azad Kashmir, Pakistan*
*[5]YFL (Yonsei Frontier Lab), Yonsei University, Seoul, Korea*
*[6]Department of Civil and Environmental Engineering, King Fahd University of Petroleum & Minerals, 31261 Dhahran, Eastern Province, Saudi Arabia*

(*Received July 15, 2020, Revised November 28, 2020, Accepted November 29, 2020*)

**Abstract.** In present article, utilizing the Love shell theory with volume fraction laws for the cylindrical shells vibrations provides a governing equation for the distribution of material composition of material. Isotopic materials are the constituents of these rings. The position of a ring support has been taken along the radial direction. The Rayleigh-Ritz method with three different fraction laws gives birth to the shell frequency equation. Moreover, the effect of height- and length-to-radius ratio and angular speed is investigated. The results are depicted for circumferential wave number, length- and height-radius ratios with three laws. It is found that the backward and forward frequencies of exponential fraction law are sandwich between polynomial and trigonometric laws. It is examined that the backward and forward frequencies increase and decrease on increasing the ratio of height- and length-to-radius ratio. As the position of ring is enhanced for clamped simply supported and simply supported-simply supported boundary conditions, the frequencies go up. At mid-point, all the frequencies are higher and after that the frequencies decreases. The frequencies are same at initial and final stage and rust itself a bell shape. The shell is stabilized by ring supports to increase the stiffness and strength. Comparison is made for non-rotating and rotating cylindrical shell for the efficiency of the model. The results generated by computer software MATLAB.

**Keywords:** MATLAB; isotropic material; boundary condition; position of ring

## 1. Introduction

The shells are basic parts in structuring different devices in engineering and technology and so on. Study of vibration characteristics of rotating cylindrical shells is a widely area of research in applied mathematics and theoretical mechanics. Analytical investigation of vibrations of these shells is performed to estimate the probable dynamical response. Variations in the shell physical parameters are inducted to enhance their strength and stability.

Addition of more physical parameters may give rise more instability in a system of a rotating cylindrical shell. During the recent years, study of rotating cylindrical shell with ring supports has gained the attention of researchers doing work on the vibration characteristics. Advanced composite materials keep extreme particular stiffness, strength and are resistant to corrosion. The problem is generated to investigate the vibrations of waves produced in water, noise and fluid flow in pipes. In the seventeenth century a thin pressure vessel in the form of a cylinder was structured and extended for industrial aims during the period: 1745-50. Investigation of vibrations for cylindrical shells was introduced by Sophie Germaine in 1821. After her research, this problem was studied by Rayliegh (1884) in the last years of the nineteenth century. The first shell theory using Kirchhoff's hypotheses for plates was given by Love (1888). After that, this theory became a foundation stage for building new ones by changing physical terms expressions. Srinivasan and Lauterbach (1971) conducted the research on isotropic long rotating cylindrical shells including influence of coriolis actions on their travelling modes. Loy and Lam (1997) investigated the shell vibrations with ring supports that restricted the motion of Cylindrical Shells (CSs) in the transverse direction. This influence was inducted by the polynomial functions. Bryan (1890) is considered to be the primer research worker who examined studied vibrations of rotating cylindrical shells. The free vibrations of a rotating ring were related with those of these shells. Zhang (2001) studied vibrations of CSs submerged in a fluid. It was seen that the fluid factor impressed vibration shell frequencies to a significant limit. Akbaş and Kocatürk (2013) investigated the post-buckling behavior of functionally graded beams under the influence of temperature loading by using total Lagrangian finite

*Corresponding author, Ph.D., Assistant Professor,
E-mail: am.khadimallah@gmail.com;
mohamedamine.khadimallah@fsgf.rnu.tn


http://www.techno-press.org/?journal=journal=anr&subpage=5 ISSN: 2287-237X (Print), 2287-2388 (Online)

element model of three-dimensional continuum approximations. Ansari and Rouhi (2015) performed nonlocal model for the frequencies of multi-walled carbon nanotubes with small effects subject to various Boundary Conditions (BCs) using Rayleigh-Ritz technique. The governing equation was formulated based on Flügge's and nonlocal shell theory. Some new resonant frequencies were identified with the association of vibrational modes and circumferential modes into shell model. Mehar *et al*. (2016) investigated the free vibration behavior of functionally graded carbon nanotube reinforced composite plate under elevated thermal environment. The carbon nanotube reinforced composite plate has been modeled mathematically using higher order shear deformation theory. Xiang *et al*. (2002) formed some closed form solution functions for studying vibrations of cylindrical shells. The mid-way ring supports were clamped around the shells. Akbaş (2015) studied the effect of material-temperature dependent on the wave propagation of a cantilever beam composed of Functionally Graded Material (FGM) under the effect of an impact force. The beam is excited by a transverse triangular force impulse modulated by a harmonic motion. Di Taranto and Lessen (1964) investigated the vibrations of thin isotropic and infinite long rotating cylindrical shells. Wang *et al*. (1997) scrutinized the vibrations of ring-stiffened CSs using Ritz polynomial functions. Materials of both shells and rings were of isotropic nature. These shells were stiffened with isotropic rings having three forms of locations on the shell outer surface. Kar and Panda (2017) analyzed the nonlinear free vibration responses of functionally graded curved (cylindrical, elliptical and hyperbolic) shell panels under heat conduction. For the present investigation, the effective material properties are evaluated through the power-law distribution using Voigt's micromechanical model. Akbaş (2017) conducted the free vibration analysis of edge cracked cantilever microscale beams composed of FGM based on the Modified Couple Stress Theory (MCST). Chung *et al*. (1981) investigated the vibrations of fluid-filled CSs and presented an analysis of experimental and analytical investigation. Penzes and Kraus (1972) applied generalized end conditions to analyze vibrations of rotating cylindrical shells. The analysis of rotating shells was confined to some special cases owing to need of approximate approach and calculation process. With powerful numerical methodologies, shell vibration analysis has completely revolutionized by advanced computers. Ramteke *et al*. (2019a) proposed to develop a geometrical model for the analysis and modelling of the uniaxial functionally graded structure using the higher-order displacement kinematics with and without the presence of porosity including the distribution. Akbaş (2018a, b, c) investigated the forced vibration analysis of sandwich deep beams made of FGM in face layers and a porous material in core layer. The FGM sandwich deep beam is subjected to a harmonic dynamic load. The FGM in the face layer is graded though the layer thickness. In order to get more realistic result for the deep beam problem, the plane solid continua and Newton-Raphson iteration method is used in the modeling of composite beam. Najafizadeh and Isvandzibaei (2007) applied ring supports to CSs for vibration analysis of along the tangential direction and founded their research on angular deformation theory of higher order. The angular deformation was used for shell equations and determined the effects of constituent volume fractions and shell configurations on the shell vibrations. FG material parameters were changed step by step. Akbaş (2018d, e, f) used the nonlinear model of the laminated beam, total Lagrangian finite element model in conjunction with the Timoshenko beam theory. The considered nonlinear problem is solved considering full geometric nonlinearity by using incremental displacement-based finite element method. The thermal post-buckling analysis of a laminated composite beam is studied under uniform temperature rising with temperature dependent physical properties. The beam is pinned at both ends and immovable ends.

Amabili *et al*. (1998) used Donnell's shallow-shell model with the quiescent, dense, inviscid and incompressible fluid. Also, the dense fluid is studied for the influence of both the internal and external side of the shell. In the external side of the shell, the fluid was considered as an unbounded domain in the radial direction, while internally, the shell was considered as filled completely. Wang and Lai (2000) examined a novel approach for the evaluation of eigen-frequencies of cylindrical shells. The numerical process adopted by them was alike the Wave Propagation Approach (WPA). Mehar *et al*. (2019) reported the buckling load parameters of the graded nanotube sandwich structure under the influence of uniform thermal loading. The corresponding properties of the graded nanotube sandwich evaluated via the extended rule of mixture including temperature dependent properties of each constituent. Akbaş (2019a, b) presented the forced vibration analysis of sandwich deep beams made of FGM in face layers and a porous material in core layer. The FGM sandwich deep beam is subjected to a harmonic dynamic load. The FGM in the face layer is graded though the layer thickness. In order to get more realistic result for the deep beam problem, the plane solid continua are used in the modeling of The FGM sandwich deep beam. Sharma *et al*. (2019) studied the functionally graded material using sigmoid law distribution under hygrothermal effect. The Eigen frequencies are investigated in detail. Frequency spectra for aspect ratios have been depicted according to various edge conditions.

Shah *et al*. (2009) and Sofiyev and Avcar (2010) studied the stability of CSs based on Rayleigh-Ritz and Galerkin technique using elastic foundations. The structures of cylindrical shell are tackled under the exponential law and axial load. Ramteke *et al*. (2020a) obtained the finite element solutions of static deflection and stress values for the functionally graded structure considering variable grading patterns (power-law, sigmoid and exponential) including the porosity effect. Naeem *et al*. (2013) conducted the vibrational behavior of submerged FG-CSs. The problem of submerged cylindrical shells was frequently met where fluid envelopes a structure. Ergin and Temarel (2002) did a vibration study of cylindrical shells. The shells lied in a horizontal direction and contained fluid and submerged in

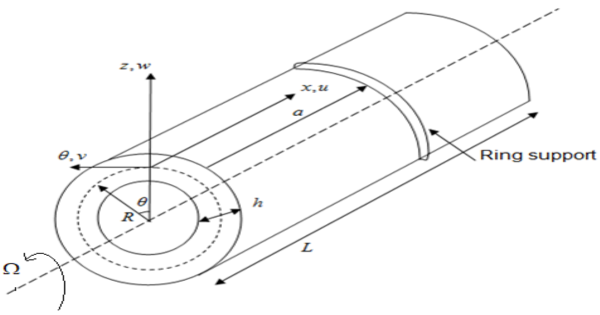


Fig. 1 Mechanical model of rotating cylindrical shell

it. Ramteke *et al*. (2020b) developed the two directional graded structure using a commercial FE package ANSYS and the subsequent deflection responses are obtained. Additionally, the model includes the porosity within the graded structure considering even type of distribution pattern. Goncalves and Batista (1988) gave an analytical investigation of submerged CSs with fluid. Sewall and Naumann (1968) considered the vibration analysis of CSs based on analytical and experimental methods. The shells were strengthened with longitudinal stiffeners. Sharma *et al*. (1998) determined frequencies of composite cylindrical shells containing fluid. They estimated the axial modal deformations by trigonometric functions. Jiang and Olson (1994) recommended the characteristics of analysis of stiffened shell using finite element method to diminish large computational efforts which are required in the conventional finite element analysis. Recently some researcher used different methods for nonlinear modeling (Eltaher *et al*. 2019, Ebrahimi *et al*. 2019, Safaei *et al*. 2019, Shahsavari *et al*. 2019, Benmansour *et al*. 2019, Mehar *et al*. 2020a, b, Akbaş 2019c, d, e, Civalek 2020).

In current study paper, utilizing the Rayleigh-Ritz Method (RRM) with polynomial, exponential and trigonometric volume fraction laws for isotropic shell vibrations. Effects of different parameters for ratios of length- and height-to-radius and angular speed versus fundamental natural frequencies been determined for isotropic cylindrical shells with clamped-free edge condition. By increasing different value of height-to-radius ratio, the resulting backward and forward frequencies increase and frequencies decrease on increasing length-to-radius ratio. Moreover, on increasing the rotating speed, the backward frequencies increase and forward frequencies decreases. The frequencies are same when the cylinder is stationary. The results generated furnish the evidence regarding applicability of present shell model and also verified by earlier published literature.

## 2. Theoretical formulations

An orthogonal system ($x$, $\theta$, $t$) is setup for the reference surface (middle surface). The $x$, $\theta$ co-ordinates are assumed to be along longitudinal and circumferential direction, respectively and $z$-co-ordinates are taken in its radial directions. The space of the ring-stiffeners $q$ on the tube may or may not have equal spaces. From one end of the isotropic cylindrical shell, the measurement of the $k^{th}$ stiffener is positioned at $x = a_k L$ with width $b_k$ and rectangular cross section depth $d_k$.

The stiffeners may be assembled from diverse materials and also from the parent tube material. $v_k$, $G_k$, $E_k$, $\rho_k$ stand for Poisson's ratio, shear modulus, Young's modulus and stiffener's mass density, respectively.

The following form for strain energy $S$ of vibrating CS is as

$$S = \frac{1}{2}\int_0^L \int_0^{2\pi} \{\varepsilon\}^T [T] \{\varepsilon\} R d\theta dx \tag{1}$$

where

$$[\varepsilon]^T = [e_1, e_2, \gamma, \kappa_1, \kappa_2, 2\tau],$$
$$[T] = \begin{pmatrix} A & B \\ C & D \end{pmatrix}$$

After substituting $\{\varepsilon\}^T$ and $[T]$ in Eq. (1), the strain energy can be written as the new form of strain energy is obtained

$$S = \frac{R}{2}\int_0^L \int_0^{2\pi} \begin{pmatrix} A_{11}e_{11}^2 + 2e_1e_2A_{12} + 2e_1k_1B_{11} \\ +2e_1k_2B_{12} + e_2^2A_{22} + 2e_2k_2B_{12} \\ +2e_2k_2B_{22} + \gamma^2A_{66} + 4\tau\gamma B_{66} + \\ k_1^2D_{22} + 2k_1k_2D_{12} + k_2^2D_{22} \\ +4\tau^2D_{66} \end{pmatrix} d\theta dx \tag{2}$$

For vibration of cylindrical shell, the Kinetic energy is

$$K = \frac{1}{2}\int_0^L \int_0^{2\pi} \rho_T \begin{bmatrix} \left(\frac{\partial u}{\partial t}\right)^2 + \left(\frac{\partial v}{\partial t} + \Omega(R+w)\right)^2 \\ + \left(\frac{\partial w}{\partial t} - \Omega v\right)^2 \end{bmatrix} R d\theta dx \tag{3}$$

The mass density relation $\rho_T$ is expressed as

$$\rho_T = \int_{-\frac{h}{2}}^{\frac{h}{2}} \rho dz \tag{4}$$

Vibrations of rotating isotropic cylindrical shells are inspected for three volume fraction laws viz.: polynomial, exponential and trigonometric. These rules control the thickness of cylindrical shell in radius direction.

Polynomial rule (Index rule-I)

$$V_f = \left(\frac{z}{h} + \frac{1}{2}\right)^{\int} \tag{5}$$

Exponential Rule (Index rule-II)

$$V_f = 1 - e^{-\left(\frac{2}{h}+\frac{1}{2}\right)^{\int}} \tag{6}$$

Trigonometric rule (Index rule-III)

$$V_{f1} = cos^2\left[\left(\frac{2}{h}+\frac{1}{2}\right)^{\int}\right] \tag{7}$$

$$V_{f2} = sin^2\left[\left(\frac{2}{h}+\frac{1}{2}\right)^{\int}\right] \tag{8}$$

The term $V_f$ is designated as total volume fraction of isotropic CS, respectively. The power exponent is denoted as $\int$ and $h$ for thickness and $z$ is the coordinate which varies from zero to infinity.

Here, Sander's theory is used for the relation of strain and curvature displacement and strain energy $S$ in modified form can be elaborated as

$$\begin{aligned} S = \frac{R}{2}\int_0^L\int_0^{2\pi}[A_{11}\left(\frac{\partial u}{\partial x}\right)^2 + \frac{A_{22}}{R^2}\left(\frac{\partial v}{\partial \theta}-w\right)^2 + \frac{2A_{12}}{R}\times \\ \left(\frac{\partial u}{\partial x}\right)\left(\frac{\partial v}{\partial \theta}-w\right) + A_{66}\left(\frac{\partial v}{\partial x}+\frac{1}{R}\frac{\partial u}{\partial \theta}\right)^2 + 2B_{11}\frac{\partial u}{\partial x}\frac{\partial^2 w}{\partial x^2} \\ +\frac{2B_{12}}{R^2}\left(\frac{\partial^2 w}{\partial \theta^2}+w\right)\left(\frac{\partial u}{\partial x}\right) + \frac{2B_{12}}{R}\left(\frac{\partial^2 w}{\partial x^2}\right)\left(\frac{\partial v}{\partial \theta}-w\right) \\ +\frac{2B_{22}}{R^3}\left(\frac{\partial v}{\partial \theta}-w\right)\left(\frac{\partial^2 w}{\partial \theta^2}+w\right) + B_{66}\left(\frac{\partial^2 w}{\partial x\partial \theta}+\frac{3}{4}\frac{\partial v}{\partial x}\right. \\ \left.-\frac{1}{4R}\frac{\partial u}{\partial \theta}\right)\left(\frac{\partial v}{\partial x}+\frac{1}{R}\frac{\partial u}{\partial \theta}\right) + D_{11}\left(\frac{\partial^2 w}{\partial x^2}\right)^2 + \frac{D_{22}}{R^4}\times \\ \left(\frac{\partial^2 w}{\partial \theta^2}+w\right)^2 + \frac{2D_{12}}{R^2}\frac{\partial^2 w}{\partial x^2}\left(\frac{\partial^2 w}{\partial \theta^2}+w\right) + 4D_{66}\times \\ \left(\frac{\partial^2 w}{\partial x\partial \theta}+\frac{3}{4}\frac{\partial v}{\partial x}-\frac{1}{4R}\frac{\partial u}{\partial \theta}\right)^2]d\theta dx \end{aligned} \tag{9}$$

For the $k^{th}$ ring-stiffener the strain energy $S_k$ is given by Galletly (1955)

$$\begin{aligned} S_k = \int_0^{2\pi}\{\frac{E_k I_{zk}}{2(R+e_k)}\left(\frac{\partial w_k}{\partial x}+\frac{1}{R+e_k}\frac{\partial^2 u_k}{\partial \theta^2}\right)^2 \\ +\frac{E_k I_{xk}}{2(R+e_k)^3}\left(w_k+\frac{\partial^2 w_k}{\partial \theta^2}\right)^2 + \frac{E_k A_k}{2(R+e_k)}\left(\frac{\partial v_k}{\partial \theta}-w_k\right)^2 \\ +\frac{G_k J_k}{2(R+e_k)}\left(-\frac{\partial^2 w_k}{\partial x\partial \theta}+\frac{1}{R+e_k}\frac{\partial u_k}{\partial \theta}\right)^2\}d\theta \end{aligned} \tag{10}$$

where $e_k$ denote the eccentricity of ring stiffener and for externally eccentric stiffener it is expressed as

$$e_k = \frac{(h+d_k)}{2} \tag{11}$$

Whereas for concentric stiffener, it is zero.

$$e_k = 0 \tag{12}$$

For internally eccentric stiffener, it is given by

$$e_k = -\frac{(h+d_k)}{2} \tag{13}$$

$I_{zk}$, $I_{xk}$ is the second moment of areas and $A_k$, $J_k$ signify the cross-section areas and torsional constant given by following equations.

$$\begin{aligned} I_{zk} = \frac{b_k^3 d_k}{12}, \quad I_{xk} = \frac{b_k d_k^3}{12} \\ A_k = b_k d_k \\ J_k = \frac{1}{3}\left[1-\frac{192 b_k}{\pi^5 d_k}\sum_{n=1,3,5}^{\infty}\frac{1}{n^5}tanh\frac{n\pi d_k}{2b_k}\right]b_k^3 d_k \end{aligned} \tag{14}$$

The kinetic energy of $k^{th}$ stiffener i.e., $K_k$ is given by

$$\begin{aligned} K_k = \frac{1}{2}\rho_k\int_o^{2\pi}\{A_k\left[\left(\frac{\partial u_k}{\partial t}\right)^2 + \left(\frac{\partial v_k}{\partial t}+\Omega(R+w)\right)^2 \right. \\ \left. +\left(\frac{\partial w_k}{\partial t}-\Omega v\right)^2\right] \\ +(I_{xk}+I_{zk})\left(\frac{\partial^2 w_k}{\partial t\partial x}\right)^2\}(R+e_k)d\theta \end{aligned} \tag{15}$$

At the position of the stiffener the associations between the displacements ($u_k$, $v_k$, $w_k$) of the $k^{th}$ stiffener and the displacements ($u$, $v$, $w$) of the tube at $x = a_k L$, from geometrical considerations, are expressed as

$$\begin{aligned} u_k = u + e_k\frac{\partial w_k}{\partial x} \\ v_k = v\left(1+\frac{e_k}{R}\right) + \frac{e_k}{R}\frac{\partial w}{\partial \theta} \\ w_k = w \end{aligned}$$

The Lagrangian functional can be obtained with the coalescence energies (strain and kinetic) with the combination of $k^{th}$ stiffener in the following shape.

$$\Pi = \left[K+\sum_{k=1}^{q}K_k\right] - \left[S+\sum_{k=1}^{q}S_k\right] \tag{16}$$

The Modal displacement form can be written as

$$\begin{aligned} u(x,\theta,t) = A_m U(x)\sin(n\theta)\cos(\omega t) \\ v(x,\theta,t) = B_m V(x)\cos(n\theta)\cos(\omega t) \\ w(x,\theta,t) = C_m W(x)\sin(n\theta)\cos(\omega t) \end{aligned} \tag{17}$$

where $A_m$, $B_m$, $C_m$ designated as the displacement amplitudes in $x$, $\theta$ and $z$ directions. The angular frequency and circumferential wave number are represented by $\omega$ and $n$ respectively. The Lagrangian energy functional $\Pi$ is framed by adding energy expressions for the cylindrical shell and ring stiffeners. The tube frequency equation is solved to extract the tube frequency and mode shapes.

$$\Pi = K + \sum_{k=1}^{q}(K_k) - \left[S+\sum_{k=1}^{q}(S_k)\right] \tag{18}$$

The assumed forms of $u$, $v$, $w$ in the Eq. (17) and the values of their partial derivatives are substituted in Eqs. (9), (10) and (15) for energy expressions $S$, $K$, $S_k$ and $K_k$, respectively and we get the eigen value, various algebraic calculations given in full form as follow

Table 1 Theoretical and existing values in the reference (Shah *et al*. 2009)

| $n$ | $m$ | Shah *et al*. (2009) | Present |
|---|---|---|---|
| 2 | 1 | 2043.77 | 2046.4 |
| | 2 | 5635.37 | 5637.1 |
| | 3 | 8932.46 | 8933.4 |
| | 4 | 11407.4 | 11407.7 |
| | 5 | 13253.1 | 13253.0 |
| 3 | 1 | 2195.05 | 2199.0 |
| | 2 | 4035.55 | 4041.2 |
| | 3 | 6614.63 | 6619.2 |
| | 4 | 9121.10 | 9124.1 |
| | 5 | 11358.91 | 11360.8 |

Table 2 Theoretical and existing values in the reference (Sewall and Naumann 1968)

| $N$ | Sewall and Naumann (1968) | Present |
|---|---|---|
| 4 | 287.0 | 287.59 |
| 5 | 203 and 211 | 201.85 |
| 6 | 175 | 166.59 |
| 7 | 163 and 169 | 166.22 |
| 8 | 188 | 189.29 |
| 9 | 224 | 226.88 |
| 10 | 268 | 274.09 |
| 11 | 326 | 328.64 |
| 12 | 382 and 385 | 389.49 |
| 13 | 440 | 456.21 |
| 14 | - | 528.57 |
| 15 | 590 | 606.45 |

Table 3 Theoretical and existing values in the reference (Arnold and Warburton 1953)

| $n$ | $m$ | Arnold and Warburton (1953) | Present |
|---|---|---|---|
| 2 | 1 | 2046.8 | 2043.77 |
| | 2 | 5637.6 | 5635.37 |
| | 3 | 8935.3 | 8932.46 |
| | 4 | 11405 | 11407.4 |
| | 5 | 13245 | 13253.1 |
| 3 | 1 | 2199.3 | 2195.05 |
| | 2 | 4041.9 | 4035.55 |
| | 3 | 6620.6 | 6614.63 |
| | 4 | 9124.0 | 9121.10 |
| | 5 | 11357.0 | 11358.91 |

$$\left[[[S]+[S_k]]-\omega^2[[K]+[K_k]]\right]X=[0] \text{ or}$$
$$[[C]-\omega^2[D]]X=[0],\quad [C]=[[S]+[S_k]]$$
$$[D]=[[K]+[K_k]]$$

Table 4 Experimental and existing values in the reference (Naeem and Sharma 2000)

| $N$ | Naeem and Sharma (2000) | Present |
|---|---|---|
| 4 | 287.59 | 288.49 |
| 5 | 201.85 | 202.33 |
| 6 | 166.59 | 166.56 |
| 7 | 166.22 | 165.63 |
| 8 | 189.29 | 188.15 |
| 9 | 226.88 | 225.26 |
| 10 | 274.09 | 271.99 |
| 11 | 328.64 | 326.03 |
| 12 | 389.49 | 386.37 |
| 13 | 456.21 | 452.53 |
| 14 | 528.57 | 524.28 |
| 15 | 606.45 | 601.51 |

Table 5 Theoretical and existing rotating values in the reference (Chen *et al*. 1993)

| $\Omega$ (rps) | 2 | Chen *et al*. (1993) | | Present | |
|---|---|---|---|---|---|
| | | $\eta_b$ | $\eta_f$ | $\eta_b$ | $\eta_f$ |
| 0.05 | 4 | 0.00840627 | 0.0083971 | 0.00840629 | 0.00839721 |
| 0.1 | 4 | 0.0084110 | 0.00839262 | 0.00841112 | 0.00839289 |
| 0.1 | 5 | 0.0135949 | 0.01357991 | 0.01359505 | 0.01358020 |
| 1.0 | 4 | 0.00849450 | 0.00831284 | 0.00852203 | 0.00834037 |
| 1.0 | 5 | 0.01366284 | 0.01351436 | 0.01369199 | 0.01354351 |

## 3. Results and discussion

The mentioned comparisons of analytical results are utilized for an efficient, valid and yields accurate results of shell vibration problems. The present theoretical results are compared with the results of Refs (Shah *et al*. 2009, Sewall and Naumann 1968) as shown in Tables 1 and 2. In Tables 3 and 4, the numerical frequencies are compared with theoretical and experimental study of Arnold and Warburton (1953) and Naeem and Sharma (2000). An excellent agreement has been seen between two sets of frequency parameters. In Table 3, the numerical frequencies are compared for simply supported-simply supported shell ends conditions with Arnold and Warburton (1953). Table 5 shows the rotating frequency comparison with Chen *et al*. (1993). Consequently, it is concluded from the above comparisons that the present procedure gives accurate results and is valid, efficient to solve the present shell problem. This is an eigenvalue problem and is resolved by the help of the MATLAB software. MATLAB software is very helpful and capable tool that gives a quick solution of the problem. Solutions of the above problem are evaluated by utilizing MATLAB software. This is a very expedient and powerful package to manage numerical problems. Application of this programming provides both eigenvalues and eigenvector very fast. The solution of the shell

Table 6 Circumferential wave number-frequency of rotating cylindrical shell ($m$ = 1, $L$ = 2, $h$ = 0.001, $R$ = 1, $\int$ = 0.5, $\Omega$ = 2.5 rps, $a$ = 1$L$)

| $n$ | C-S | | S-S | |
|---|---|---|---|---|
| | $\eta_b$ | $\eta_f$ | $\eta_b$ | $\eta_f$ |
| 1 | 627.7201 | 627.6070 | 617.4430 | 617.3298 |
| 2 | 427.8638 | 427.7556 | 420.8590 | 420.7507 |
| 3 | 286.6320 | 286.5414 | 281.9396 | 281.8490 |
| 4 | 196.9106 | 196.8362 | 193.6872 | 193.6128 |
| 5 | 140.5404 | 140.4785 | 138.2399 | 138.1781 |
| 6 | 104.3337 | 104.2812 | 102.6263 | 102.5738 |
| 7 | 80.4752 | 80.4299 | 79.15903 | 79.11372 |
| 8 | 64.5955 | 64.5557 | 63.54029 | 63.50051 |
| 9 | 54.3031 | 54.2676 | 53.41817 | 53.38275 |
| 10 | 48.2867 | 48.2547 | 47.50288 | 47.47097 |

Table 7 Circumferential wave number –frequency rotating cylindrical shell ($m$ = 1, $L$ = 2, $h$ = 0.001, $R$ = 1, $\int$= 0.5, $\Omega$ = 2.5 rps, $a$ = 1$L$)

| $n$ | C-S | | S-S | |
|---|---|---|---|---|
| | $\eta_b$ | $\eta_f$ | $\eta_b$ | $\eta_f$ |
| 1 | 564.2589 | 564.1236 | 555.0208 | 554.8856 |
| 2 | 354.5830 | 354.4664 | 348.7781 | 348.6616 |
| 3 | 224.1601 | 224.0664 | 220.4906 | 220.3969 |
| 4 | 148.2998 | 148.2243 | 145.8723 | 145.7969 |
| 5 | 103.4221 | 103.3599 | 101.7295 | 101.6674 |
| 6 | 75.79866 | 75.74622 | 74.55862 | 74.50619 |
| 7 | 58.28900 | 58.24379 | 57.33637 | 57.29116 |
| 8 | 47.26522 | 47.22555 | 46.49444 | 46.45477 |
| 9 | 40.88898 | 40.85366 | 40.22480 | 40.18949 |
| 10 | 38.15244 | 38.12062 | 37.53608 | 37.50426 |

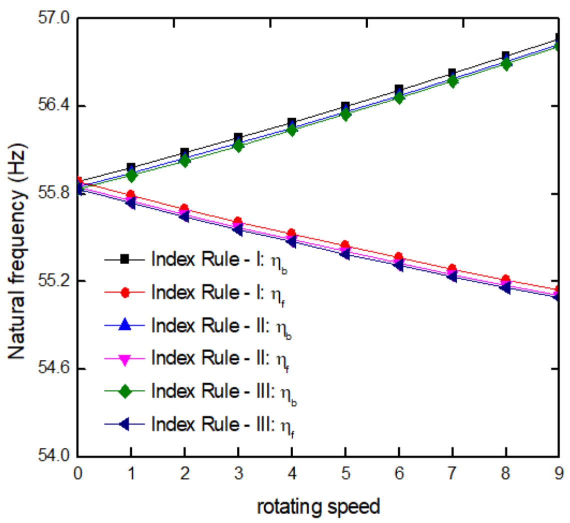


Fig. 2 Relationship between natural frequency and angular speed $\Omega$ with fraction laws for Form-I C-S rotating isotropic cylindrical shell

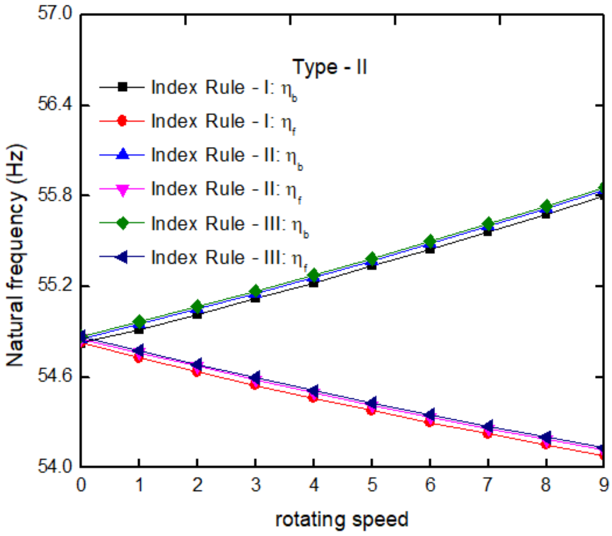


Fig. 3 Relationship between natural frequency and angular speed $\Omega$ with fraction laws for Form-I S-S rotating isotropic cylindrical shell ($m$ = 1, $n$ = 3, $h/R$ = 0.03, $L/R$ = 10, $\int$ = 30, $a$ = 1$L$)

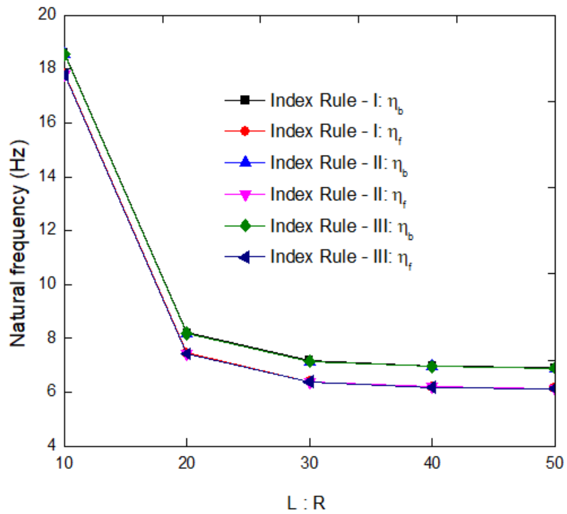


Fig. 4 Relationship between natural frequency and $L/R$ with fraction laws for C-S rotating isotropic cylindrical shell ($m$ = 1, $n$ = 2, $h/R$ = 0.01, $\int$ = 0.5, $\Omega$ = 2.5 rps, $a$ = 1$L$)

frequency equation consists of six roots. From these six roots, the minimum absolute real values are selected. When a shell sets into rotation, two eigen-solution occurs, i.e., one is positive (backward, $\Omega$ > 0) and other is negative (forward, $\Omega$ < 0). These two frequencies are similar when the shell vibrates but static. From numerical values of the frequencies, the forward frequencies are lower than that of backward wave.

Tables 6 and 7 shows the rotating frequencies versus $n$ (wave number) and $m$ (axial wave mode) with ring supports $a$ = 1$L$. The frequencies for backward and forward waves increase indefinitely as $n$ and $m$ grows for isotropic CSs.

Figs. 2 and 3 sketched for the frequency variations versus angular speed for C-S and S-S cylindrical shells.

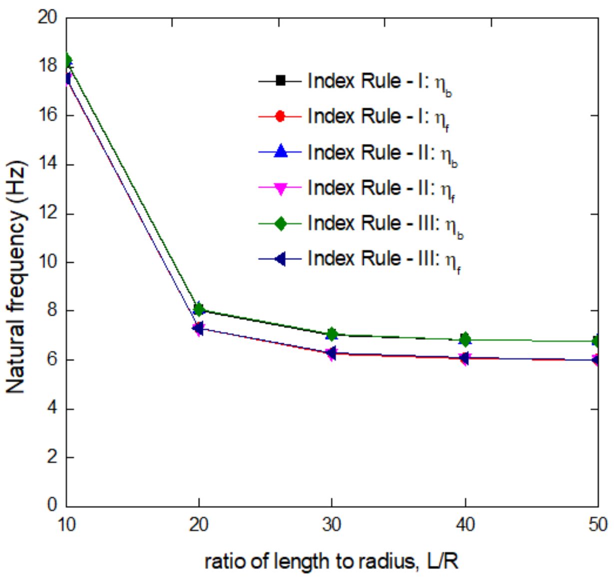


Fig. 5 Relationship between natural frequency and *L*/*R* with fraction laws for S-S rotating isotropic cylindrical shell

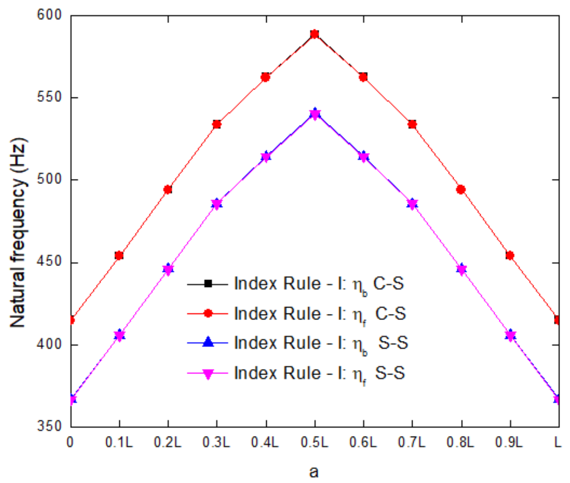


Fig. 6 Relationship between natural frequency and ring supports with index rule-I for S-S rotating isotropic cylindrical shell

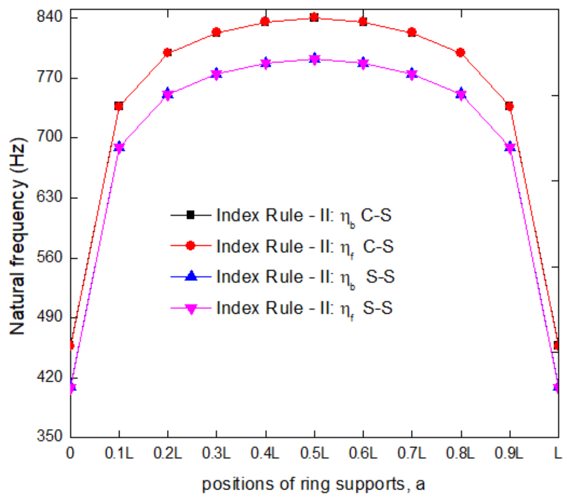


Fig. 7 Relationship between natural frequency and ring supports with index rule-II for S-S rotating isotropic cylindrical shell

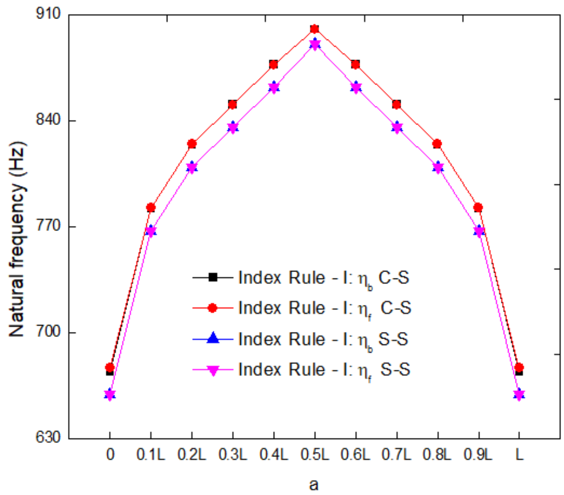


Fig. 8 Relationship between natural frequency and ring supports with index rule-III for S-S rotating isotropic cylindrical shell

These variations of frequencies are drawn with three volume fraction laws. These frequencies have been examined for the wave number, $m$ = 1, $n$ = 3, $h/R$ = 0.03, $L/R$ = 10, $\int$ = 30, $a$ = 1$L$. These variations of the natural frequency (Hz) have been calculated for the volume fraction fraction rules i.e., Index rule-I (polynomial rule), Index rule-II (exponential rule), Index rule-III (trigonometric rule). The speed of rotating cylinder is varied from $\Omega$ = 0~9. The frequencies at $\Omega$ = 0 are same due to no rotation in cylinder. After that for other values of $\Omega$ (= 0~9), the rotation frequencies exist. The frequencies bifurcate into two parts, one is backward ($\eta_b$) and other is forward ($\eta_f$). The backward frequencies ($\eta_b$) increase on increasing the rotating speed $\Omega$ (= 0~9) and the forward frequencies ($\eta_f$) for said range of rotating speed is in the form of decreasing. In these figures, for S-S, variations of frequencies are lower than that of C-S frequencies. The symmetry of these index rules is expressed as Index rule-I > Index rule-II > Index rule-III. Figs. 4 and 5 shows the variations of natural frequencies (Hz) versus $L/R$. It is noted that the frequencies reduce as $L/R$ is enhanced with the position of the ring ($a$ = 0.4 L) and $h/R$ = 0.01. The shell has been placed on simply supports i.e., simply support edge conditions taken into consideration. The cylinder rotates with speed ($\Omega$ = 2.5 rps). The backward and forward frequencies for $L/R$ (= 10) are 18.843, 17.945 (Index rule-I), 18.764, 17.826 (Index rule-II), 18.652, 17.659 for Form-I and for Form-II, the frequencies are 18.587, 17.860 (Index rule-I), 18.436, 17.739 (Index-rule-II), 18.319, 17.650. It can be seen that the frequency results of Index rule-II are composed between the Index rule-I and Index rule-III. Moreover, it is observed that the Form-I frequencies are larger than that of Form-II frequencies.

Figs. 6-8 show the frequency response of isotropic cylindrical shell against ring positions with $L/d$ = 5, $h/R$ = 0.003 and ∫ = 0.7. As $a$ is enhanced for prescribed boundary conditions, the frequencies go up. At $a$ (= 0.5$L$), the frequencies are higher and at $a$ (= 0.6$L$~0.9$L$), the frequencies decrease. The frequencies are same at $a$ = 0, 1 and rust itself a bell shape. It can be seen that the exponential law is sandwiched between BCs C-S and S-S. The frequency of C-S is higher than that of S-S. As shown by this figure, the polynomial laws have the highest frequency curves. These frequencies have a great impact on the vibration of isotropic CSs.

## 4. Conclusions

In this article, the rotating frequency characteristics of shell is investigated with volume fraction law according to Rayleigh-Ritz technique the ring supports are located at various positions along the axial direction round the shell circumferential direction. For two conditions, frequency variations show different behavior with these values of polynomial, exponential and trigonometric laws. The influence of the positions of ring supports for clamped simply end conditions is very visible than simply supported condition. These results have been obtained for circumferential wave mode, ratios of length- and- thickness-to-radius. Variations of frequencies with the locations of ring supports have been analyzed placed round the circumferential direction. The position of a ring support has been taken along the shell length. It is seen that frequencies increases on inducting of ring-stiffeners. As the position of a ring is changed from one end of the shell to other one, the frequency first increases and obtains its maximum value at the shell mid length position and then decreases. Its values at both ends are similar. The present problem can be extended for vibration of rotating carbon nanotubes with fraction laws.

## Declaration of conflicting interests

The author(s) declared no potential conflicts of interest with respect to the research, authorship, and/or publication of this article.

## Acknowledgments

This project was supported by the Deanship of Scientific Research at Prince Sattam Bin Abdulaziz University under research project no. 2020/01/16794.

## References

Akbaş, Ş.D. (2015), "Wave propagation of a functionally graded beam in thermal environments", *Steel Compos. Struct., Int. J.*, **19**(6), 1421-1447. https://doi.org/10.12989/scs.2015.19.6.1421.

Akbaş, Ş.D. (2017), "Free vibration of edge cracked functionally graded microscale beams based on the modified couple stress theory", *Int. J. Struct. Stab. Dyn.*, **17**(3), 1750033. https://doi.org/10.1142/S021945541750033X.

Akbaş, Ş.D. (2018a), "Investigation on free and forced vibration of a bi-material composite beam", *J. Politech. Dergisi*, **21**(1), 65-73.

Akbaş, Ş.D. (2018b), "Post-buckling responses of a laminated composite beam", *Steel Compos. Struct., Int. J.*, **26**(6), 733-743. http://dx.doi.org/10.12989/scs.2018.26.6.733.

Akbaş, Ş.D. (2018c), "Nonlinear thermal displacements of laminated composite beams", *Coupled Syst. Mech., Int. J.*, **7**(6), 691-705. https://doi.org/10.12989/csm.2018.7.6.691.

Akbaş, Ş.D. (2018d), "Geometrically nonlinear analysis of a laminated composite beam", *Struct. Eng. Mech., Int. J.*, **66**(1), 27-36. http://dx.doi.org/10.12989/sem.2018.66.1.027.

Akbaş, Ş.D. (2018e), "Thermal post-buckling analysis of a laminated composite beam", *Struct. Eng. Mech., Int. J.*, **67**(4), 337-346. http://dx.doi.org/10.12989/sem.2018.67.4.337.

Akbaş, Ş.D. (2018f), "Large deflection analysis of a fiber reinforced composite beam", *Steel Compos. Struct., Int. J.*, **27**(5), 567-576. https://doi.org/10.12989/scs.2018.27.5.567.

Akbaş, Ş.D. (2019a), "Hygrothermal post-buckling analysis of laminated composite beams", *Int. J. Appl. Mech.*, **11**(1), 1950009. https://doi.org/10.1142/S1758825119500091.

Akbaş, Ş.D. (2019b), "Forced vibration analysis of functionally graded sandwich deep beams", *Coupled Syst. Mech., Int. J.*, **8**(3), 259-271. https://doi.org/10.12989/csm.2019.8.3.259.

Akbaş, Ş.D. (2019c), "Post-buckling analysis of a fiber reinforced composite beam with crack", *Eng. Fract. Mech.*, **212**, 70-80. https://doi.org/10.1016/j.engfracmech.2019.03.007.

Akbaş, Ş.D. (2019d), "Nonlinear static analysis of laminated composite beams under hygro-thermal effect", *Struct. Eng. Mech., Int. J.*, **72**(4), 433-441. https://doi.org/10.12989/sem.2019.72.4.433.

Akbaş, Ş.D. (2019e), "Nonlinear behavior of fiber reinforced cracked composite beams", *Steel Compos. Struct., Int. J.*, **30**(4), 327-336. http://dx.doi.org/10.12989/scs.2019.30.4.327.

Akbaş, Ş.D. and Kocatürk, T. (2013), "Post-buckling analysis of functionally graded three-dimensional beams under the influence of temperature", *J. Therm. Stresses*, **36**(12), 1233-1254. https://doi.org/10.1080/01495739.2013.788397.

Amabili, M., Pellicano, F. and Paidoussis M.P. (1998), "The small free vibrations and deformation of thin elastic shell", *Phil. Trans. R Soc. London*, **179**, 491-549. https://doi.org/10.1098/rsta.1888.0016.

Ansari, R. and Rouhi, H. (2015), "Nonlocal flügge shell model for the axial buckling of single-walled carbon nanotubes: An analytical approach", *Int. J. Nano Dimens.*, **6**(5), 453-462. https://doi.org/10.7508/IJND.2015.05.002.

Arnold, R.N. and Warburton, G.B. (1953), "The flexural vibrations of thin cylinders", *Proc. Inst. Mech. Eng.*, **167**(1), 62-80. https://doi.org/10.1243/PIMEPROC195316701402.

Benmansour, D.L., Kaci, A., Bousahla, A.A., Heireche, H., Tounsi, A., Alwabli, A.S., Alhebshi, A.M., Al-Ghmady, K. and Mahmoud, S.R. (2019), "The nano scale bending and dynamic properties of isolated protein microtubules based on modified strain gradient theory", *Adv. Nano Res., Int. J.*, **7**(6), 443-457. https://doi.org/10.12989/anr.2019.7.6.443.

Bryan, G.H. (1890), "On the beats in the vibration of revolving cylinder", *Proc. Cambridge Philos. Soc.*, **7**,101-111.

Chen, Y., Zhao, H.B. and Shin, Z.P. (1993), "Vibration of high speed rotating shells with calculation for cylindrical shells", *J. Sound Vib.*, **160**, 137. https://doi.org/10.1006/jsvi.1993.1010.

Chung, H., Turula, P. Mulcahy, T.M. and Jendrzejczyk, J.A. (1981), "Analysis of cylindrical shell vibrating in a cylindrical fluid region", *Nucl. Eng. Des.*, **63**(1), 109-1012. https://doi.org/10.1016/0029-5493(81)90020-0.

Civalek, Ö. (2020), "Vibration of functionally graded carbon nanotube reinforced quadrilateral plates using geometric transformation discrete singular convolution method", *Int. J. Num. Methods Eng.*, **121**(5), 990-1019. https://doi.org/10.1002/nme.6254.

Shah, A. G., Mahmood, T., and Naeem, M. N. (2009), "Vibrations of FGM thin cylindrical shells with exponential volume fraction law", Applied Mathematics and Mechanics, 30(5), 607-615. http/10.1007/s10483-009-0507-x

Di Taranto, R.A. and Lessen, M. (1964), "Coriolis acceleration effect on the vibration of rotating thin walled circular cylinder", *J. Appl. Mech. T. ASME*, **31**, 700-701. https://doi.org/ 10.1115/1.3629733.

Ebrahimi, F., Dabbagh, A., Rabczuk, T. and Tornabene, F. (2019), "Analysis of propagation characteristics of elastic waves in heterogeneous nanobeams employing a new two-step porosity-dependent homogenization scheme", *Adv. Nano Res., Int. J.*, **7**(2), 135-143. https://doi.org/10.12989/anr.2019.7.2.135.

Ergin, A. and Temarel, P. (2002), "Free vibration of a partially liquid-filled and submerged, horizontal cylindrical shell", *J. Sound Vib.*, **254**(5), 951-965. https://doi.org/10.1006/jsvi.2001.4139.

Eltaher, M.A., Almalki, T.A., Ahmed, K.I. and Almitani, K.H. (2019), "Characterization and behaviors of single walled carbon nanotube by equivalent-continuum mechanics approach", *Adv. Nano Res., Int. J.*, **7**(1), 39-49. https://doi.org/10.12989/anr.2019.7.1.039.

Galletly, G.D. (1955), "On the in-vacuo vibrations of simply supported, ring-stiffened cylindrical shells", US National Congress of Applied Mechanics, USA.

Goncalves, P.B. and Batista, R.C. (1988), "Non-linear vibration analysis of fluid-filled cylindrical shells", *J. Sound Vib.*, **127**(1), 133-143. https://doi.org/10.1006/jsvi.2001.4139.

Jiang, J. and Olson, M.D. (1994), "Vibrational analysis of orthogonally stiffened cylindrical shells using super elements", *J. Sound Vib.*, **173**, 73-83. https://doi.org/10.1006/jsvi.1994.1218.

Kar, V.R. and Panda, S.K. (2017), "Large-amplitude vibration of functionally graded doubly-curved panels under heat conduction", *AIAA J.*, **55**(12), 4376-4386. https://doi.org/10.2514/1.J055878.

Love, A.E.H. (1888), "On the small free vibrations and deformation of thin elastic shell", *Phil. Trans. R. Soc. London*, **179**, 491-549.

Loy, C.T. and Lam, K.Y. (1997), "Vibration of cylindrical shells with ring supports", *J. Mech. Eng.*, **39**, 455-471. https://doi.org/10.1016/S0020-7403(96)00035-5.

Mehar, K., Panda, S.K., Dehengia, A. and Kar, V.R. (2016), "Vibration analysis of functionally graded carbon nanotube reinforced composite plate in thermal environment", *J. Sandw. Struct. Mater.*, **18**(2), 151-173. https://doi.org/10.1177/1099636215613324.

Mehar, K., Panda, S.K., Devarajan, Y. and Choubey, G. (2019), "Numerical buckling analysis of graded CNT-reinforced composite sandwich shell structure under thermal loading", *Compos. Struct.*, **216**, 406-414. https://doi.org/10.1016/j.compstruct.2019.03.002.

Mehar, K., Panda, S.K. and Sharma, N. (2020a), "Numerical investigation and experimental verification of thermal frequency of carbon nanotube-reinforced sandwich structure", *Eng. Struct.*, **211**, 110444. https://doi.org/10.1016/j.engstruct.2020.110444.

Mehar, K., Mishra, P.K. and Panda, S.K. (2020b), "Numerical investigation of thermal frequency responses of graded hybrid smart nanocomposite (CNT-SMA-Epoxy) structure", *Mech. Adv. Mater. Struct.*, **2020**, 1-13. https://doi.org/10.1080/15376494.2020.1725193.

Moazzez, K., Googarchin, H.S. and Sharifi, S.M.H. (2018), "Natural frequency analysis of a cylindrical shell containing a variably oriented surface crack utilizing line-spring model." *Thin-Wall. Struct.*, **125**, 63-75. https://doi.org/10.1016/j.tws.2018.01.009.

Naeem, M.N. and Sharma, C.B. (2000), "Prediction of natural frequencies for thin circular cylindrical shells", *Proc. Inst. Mech. Eng.*, **214**(10), 1313-1328. https://doi.org/10.1243/0954406001523290

Naeem, M.N., Ghamkhar, M., Arshad, S.H. and Shah, A.G. (2013), "Vibration analysis of submerged thin FGM cylindrical shells", *J. Mech. Sci. Technol.*, **27**(3), 649-656. https://10.1007/s12206-013-0119-6.

Najafizadeh, M.M. and Isvandzibaei, M.R. (2007), "Vibration of (FGM) cylindrical shells based on higher order shear deformation plate theory with ring support", *Acta Mech.*, **191**, 75-91. http/10.1007/s00707-006-0438-0.

Penzes, R.L.E. and Kraus, H. (1972), "Free vibrations of pre-stresses cylindrical shells having arbitrary homogeneous boundary conditions", *AIAA J.*, **10**, 1309. https://doi.org/10.2514/3.6605.

Ramteke, P.M., Mehar, K., Sharma, N. and Panda, S. (2020a), "Numerical prediction of deflection and stress responses of functionally graded structure for grading patterns (power-law, sigmoid and exponential) and variable porosity (even/uneven)", *Sci. Iranica.*, In Press.

Ramteke, P.M., Mahapatra, B.P., Panda, S.K. and Sharma, N. (2020b), "Static deflection simulation study of 2D Functionally graded porous structure", *Mater. Today Proc.*, **33**(8), 5544-5547. https://doi.org/10.1016/j.matpr.2020.03.537.

Ramteke, P.M., Panda, S.K. and Sharma, N. (2019a), "Effect of grading pattern and porosity on the eigen characteristics of porous functionally graded structure", *Steel Compos. Struct., Int. J.*, **33**(6), 865-875. https://doi.org/10.12989/scs.2019.33.6.865.

Rayliegh, J.W.S. (1884), *Theory of Sound*, Macmillan, London, UK.

Sadoughifar, A., Farhatnia, F., Izadinia, M. and Talaeetaba, S.B. (2020), "Size-dependent buckling behaviour of FG annular/circular thick nanoplates with porosities resting on Kerr foundation based on new hyperbolic shear deformation theory", *Struct. Eng. Mech., Int. J.*, **73**(3), 225-238. https://doi.org/10.12989/sem.2020.73.3.225.

Safaei, B., Khoda, F.H. and Fattahi, A.M. (2019), "Non-classical plate model for single-layered graphene sheet for axial buckling", *Adv. Nano Res., Int. J.*, **7**(4), 265-275. https://doi.org/10.12989/anr.2019.7.4.265.

Sewall, J.L. and Naumann, E.C. (1968), *An Experimental and Analytical Vibration Study of Thin Cylindrical Shells with and without Longitudinal Stiffeners*, National Aeronautic and Space Administration, Springfield, USA.

Shah, A.G., Mahmood, T. and Naeem, M.N. (2009), "Vibrations of FGM thin cylindrical shells with exponential volume fraction law", *Appl. Math. Mech.*, **30**(5), 607-615. http/10.1007/s10483-009-0507-x.

Shahsavari, D., Karami, B. and Janghorban, M. (2019), "Size-dependent vibration analysis of laminated composite plates", *Adv. Nano Res., Int. J.*, **7**(5), 337-349. https://doi.org/10.12989/anr.2019.7.5.337.

Sharma, C.B., Darvizeh, M. and Darvizeh, A. (1998), "Natural frequency response of vertical cantilever composite shells containing fluid", *Eng. Struct.*, **20**(8), 732-737. https://doi.org/10.1016/S0141-0296(97)00102-8.

Sharma, P., Singh, R. and Hussain, M. (2019), "On modal analysis of axially functionally graded material beam under hygrothermal effect", *Proc. Inst. Mech. Eng. C J. Mech. Eng. Sci.*, **234**(5), 1085-1101. https://doi.org/10.1177/0954406219888234.

Sofiyev, A.H. and Avcar, M. (2010), "The stability of cylindrical shells containing an FGM layer subjected to axial load on the Pasternak foundation", *Engineering*, **2**, 228-236. https://10.4236/eng.2010.24033.

Srinivasan, A.V. and Luaterbach, G.F. (1971), "Travelling waves in rotating cylindrical shells", *Trans*. *ASME J*. *Eng*. *Ind*., **93**, 1229-1232. https://doi.org/10.1115/1.3428067.

Wang, C. and Lai, J.C.S. (2000), "Prediction of natural frequencies of finite length circular cylindrical shells", *Appl*. *Acoust*., **59**(4), 385-400. https://doi.org/10.1016/S0003-682X(99)00039-0.

Wang, C.M., Swaddiwudhipong, S. and Tian, J. (1997), "Ritz method for vibration analysis of cylindrical shells with ring-stiffeners", *J*. *Eng*. *Mech*., **123**, 134-143. https://doi.org/10.1061/(ASCE)0733-9399(1997)123:2(134).

Xiang, Y., Ma, Y.F., Kitipornchai, S. and Lau, C.W.H. (2002), "Exact solutions for vibration of cylindrical shells with intermediate ring supports", *Int*. *J*. *Mech*. *Sci*., **44**(9),1907-1924. https://doi.org/10.1016/S0020-7403(02)00071-1.

Zhang, X.M., Liu, G.R. and Lam, K.Y. (2001), "Coupled vibration of fluid-filled cylindrical shells using the wave propagation approach", *Appl*. *Acoust.*, **62**, 229-243. https://doi.org/10.1016/S0003-682X(00)00045-1.

*CC*